Applied Clay Science 160 (2018) 116–125

Contents lists available at ScienceDirect

Applied Clay Science

journal homepage: www.elsevier.com/locate/clay

Research paper

Porous clay heterostructures intercalated with multicomponent pillars as catalysts for dehydration of alcohols

Lucjan Chmielarz[a,*], Andrzej Kowalczyk[a], Monika Skoczek[a], Małgorzata Rutkowska[a], Barbara Gil[a], Piotr Natkański[a], Marcelina Radko[a], Monika Motak[b], Radosław Dębek[b], Janusz Ryczkowski[c]

[a] Jagiellonian University, Faculty of Chemistry, Gronostajowa 2, 30-387 Kraków, Poland
[b] AGH University of Science and Technology, Faculty of Energy and Fuels, Mickiewicza 30, 30-059 Kraków, Poland
[c] Maria Curie Skłodowska University, Faculty of Chemistry, Maria Curie-Skłodowska 2, 20-031 Lublin, Poland

ARTICLE INFO

Keywords:
Montmorillonite
Intercalation
Porous clay heterostructures
Catalysis
Acid sites
Methanol dehydration
Ethanol dehydration

ABSTRACT

Montmorillonites intercalated with silica, silica-alumina, silica-titania and silica-zirconia pillars by surfactant directed method were studied as catalysts for dehydration of methanol and ethanol to dimethyl ether as well as diethyl ether and ethylene, respectively. Moreover, the samples of montmorillonite intercalated with silica pillars were doped with aluminum using template ion-exchange method. In the case of all the samples deposited metal (Al, Ti, Zr) species were present in highly dispersed forms and resulted in generation of acid sites catalytically active in dehydration of methanol and ethanol. The best catalytic results in both studied processes were obtained for the samples doped with aluminum, especially introduced by using template ion-exchange method (first time applied for deposition of metal cations into PCHs), which were more catalytically active in the process of methanol to dimethyl ether conversion than γ-Al_2O_3 (one of the most important commercial catalysts of this process). High catalytic activity of the aluminum doped samples was related to the nature and strength of acid sites active in the processes of alcohols dehydration.

1. Introduction

Cationic layered clay minerals are a group of materials with a very high potential for possible applications in various areas, including catalysis. It is related to their unique structures, which can be relatively easy modified in various ways to adjust properties of clay minerals to specific needs. There is a great variety of clay minerals with different layered structures and containing various chemical elements important in catalysis.

Various methods were proposed for functionalization of cationic layered clay minerals for catalytic applications. Among them intercalation of cationic layered minerals with metal oxide pillars (e.g. Al_2O_3, TiO_2, ZrO_2), resulting in materials called pillared interlayered clays (PILCs), is considered as one of the most important method (Chmielarz and Kowalczyk, 2015). PILCs are characterized by a relatively high specific surface area (150–350 m^2/g), developed microporous structure, ion-exchange properties and surface acidity (Chmielarz and Kowalczyk, 2015). Porous clay heterostructures (PCHs) are another very important group of materials, which can be produced from cationic layered clay minerals (Galarneau et al., 1995). The synthesis of PCHs is based on intercalation of pure silica (Benjelloun et al., 2001) or multicomponent silica-containing pillars (Kooli et al., 2006; Chmielarz et al., 2009a) into the interlayer space of clay mineral by surfactant directed method. PCHs are characterized by a relatively high specific surface area (up to 1000 m^2/g), combined micro- and mesoporous structure, surface acidity and cation exchange properties. Acidity is a very important property of PCHs influencing their catalytic performance in various processes and is dependent mainly on the host clay mineral used for the synthesis of these materials (Pichowicz and Mokaya, 2001; Kooli et al., 2006; Chmielarz et al., 2010, 2011, 2012; Saboya et al., 2016) and cationic species (e.g. Al^{3+}, Ti^{4+} or Zr^{4+}) incorporated into silica pillars (Chmielarz et al., 2009b, 2010, 2014; Pinto et al., 2012). Another possible way for deposition of cationic species, called template ion-exchange (TIE) method (Kowalczyk et al., 2016, 2017), is based on exchange of organic templates for cationic metal species in as-synthetized PCHs in a polar solvent. The TIE method seems to be a very promising alternative for other methods of catalytically active components deposition (e.g. impregnation or grafting). This method was reported to be effective for deposition of various metal cations into mesoporous silicas, mainly of MCM-41 (Kowalczyk et al.,

---

[*] Corresponding author.
E-mail address: chmielar@chemia.uj.edu.pl (L. Chmielarz).

https://doi.org/10.1016/j.clay.2017.12.015
Received 13 July 2017; Received in revised form 20 October 2017; Accepted 10 December 2017

2016, 2017), and resulted in significant amounts of deposited metal species in highly dispersed form. According to the authors knowledge up till now the application of TIE method for deposition of catalytically active components into PCHs has not been reported in scientific literature.

PCH materials were studies as catalysts of various reactions including DeNOx process (Chmielarz et al., 2009a, 2009b, 2011; Chmielarz and Kowalczyk, 2015). Among PCHs intercalated with various pillars and doped with different transition metals the most promising results were obtained for monmorillonite intercalated with silica-titania pillars and additionally modified with copper or iron, which were able to effectively catalyse reduction of NO with ammonia in a broad temperature range with a very high selectivity to dinitrogen (Chmielarz et al., 2009a). Belver et al. (2012) reported very promising catalytic properties of delaminated porous clay heterostructures (DPCHs) intercalated with silica-alumina pillars in the synthesis of p-cymene from limonene. WO_3 supported on PCHs intercalated with Si—Zr pillars were reported as active catalysts for esterification of ricinoleic acid with 2-ethylhexanol. Moreover, authors reported that active components were not leached to the liquid phase, which indicated their high stability. On the other hand Pires et al. (2004) and Pinto et al. (2012, 2014) reported high efficiency of PCHs in separation of gas mixtures. Silica intercalated PCHs modified with zirconia presented high selectivity in separation of aromatic molecules such as toluene/benzene, *p*-xylene/benzene and benzene/*n*-hexane. Activating role of zirconium was related to its high surface acidity (Pinto et al., 2012). Moreover, PCHs were reported to be effective adsorbents of reactive dyes, Remazol Violet 5R and Acid Blue 25 (Aguiar et al., 2017). The adsorptive efficiency of PCHs was improved by their intercalation with silica-zirconia pillars. It was suggested that adsorption process takes place by electrostatic interactions between the silanol groups of PCHs with functional groups of dyes, such as amine or hydroxyl. PCHs showed to be promising materials for the adsorption of dye. On the other hand PCHs modified with amine species were reported to be effective adsorbents for the CO_2 capture (Vilarrasa-Garcia et al., 2017). It was assumed that CO_2 capture occurs by the coexistence of physical and chemical adsorption sites. This short presentation of various examples of successful applications of PCH based materials in various areas clearly shows their great potential.

The presented studies are related to the synthesis of effective catalysts based on the PCH materials for dehydration of alcohols to DME, DEE and ethylene.

Alcohols have been considered as being among the best alternatives to petroleum for the production of environmental-friendly transportation fuels, fuels additives and petrochemicals. Dimethyl ether (DME) and diethyl ether (DEE) can be produced by dehydration of methanol or ethanol, respectively, over solid acid catalysts (Varisli et al., 2007; Rownaghi et al., 2012). Dimethyl ether (DME), the simplest of ethers, is one of the most promising environmentally benign and economic alternative fuels for the future applications (Xu et al., 1997; Rownaghi et al., 2012). It is related to its high cetane number (about 55–60), high oxygen content (34.8% by mass) and lack of C—C bond (Xu et al., 1997; Takeguchi et al., 2000; Varisli et al., 2007; Rownaghi et al., 2012). DME is used as coolant, key intermediate for the production of many important chemicals (such as dimethyl sulfate or methyl acetate), source of hydrogen for fuel cells, fuel in gas turbines for power generation (Jin et al., 2007; Stiefel et al., 2011; Tokay et al., 2012). Dimethyl ether can be produced in two main routes. The first one is based on direct synthesis of DME from syngas (syngas-to-dimethyl ether, STD) over bifunctional catalysts, consisting of methanol synthesis component as well as methanol dehydration component (Xu et al., 1997; Jin et al., 2007; Stiefel et al., 2011; Rownaghi et al., 2012; Tokay et al., 2012). The second route is based on two separated processes consisting of methanol synthesis from syngas in a first step and methanol to DME conversion in the second step (methanol-to-dimethyl ether, MTD) (Xu et al., 1997; Jin et al., 2007; Stiefel et al., 2011; Rownaghi et al., 2012; Tokay et al., 2012). DME synthesis from methanol is reported to be acid catalyzed exothermic reaction. Commercial catalysts, typically used for the MTD process, are solid acid materials, such as γ-Al_2O_3, zeolites (HZSM-5 or HY), silica-alumina or phosphorus-alumina (Xu et al., 1997; Yaripour et al., 2005; Jin et al., 2007; Stiefel et al., 2011; Abu-Dahrieh et al., 2012; Rownaghi et al., 2012; Sung et al., 2012; Tokay et al., 2012; Alamolhoda et al., 2012). Dehydration of ethanol results in ethylene, which is one of the main feed stock for petrochemical industry and diethyl ether (DEE), which has excellent properties of transportation fuels (cetane number above 125) (Varisli et al., 2007; Takahara et al., 2015). Good burning properties of DEE make it a promising alternative fuel or fuel additive for diesel fuel (Kito-Borsa et al., 1998). Blending of DEE with ethanol was reported to improve the cold start problem in ethanol fueled cars (Ciftci et al., 2012).

2. Experimental

2.1. Preparation of catalysts

Bentonite (CEC = 82 cmol(+)/kg, S_{BET} = 77 m^2/g, S&B Industrial Minerals GmbH) was used as a starting material for the preparation of a series of PCHs. Montmorillonite was the main component of raw clay with only a small contribution of muscovite, illite and quartz. The raw clay was purified by sedimentation. The slurry of 3 wt% of clay in water was stirred for 2 h and then sediment in Imhoff funnel for 24 h. Subsequently, the modified clay mineral (6 g) was added to a solution (0.1 M; 200 ml) of surfactant (hexadecyltrimethylammonium chloride – HDTMA, Fluka) and stirred at 50 °C for 24 h. Then, the modified montmorillonite (HDTMA-Mont) was separated from the solution and washed with demineralized water until complete removal of chloride anions. In the next step, the modified clay was divided into four parts. Each portion of montmorillonite modified with surfactant was added to melted hexadecylamine (HDA, Fluka), which played a role of co-surfactant.

Subsequently, depending on the type of pillaring agent used, various porous clay heterostructure (PCH) materials were obtained:

2.1.1. PCH-Si

Tetraethylorthosilicate (TEOS, Fluka) was added to the first portion of montmorillonite modified with surfactant and co-surfactant. The obtained dispersion was allowed to react for 4 h under continuous stirring. The HDTMA/HDA/TEOS molar ratio of 1/20/150 was applied in the PCH-Si synthesis.

2.1.2. PCH-Al

A mixture of TEOS and aluminum isopropoxide (AIP, Fluka) was added into the second portion of montmorillonite modified with surfactant and co-surfactant. The obtained dispersion was allowed to react for 4 h under continuous stirring. The HDTMA/HDA/TEOS/AIP molar ratio of 1/20/144/6 was applied in the synthesis of PCH-Al.

2.1.3. PCH-Ti

The procedure similar to that used for the PCH-Al synthesis was applied. The only difference was related to the use of titanium isopropoxide (TIP, Fluka) apart from AIP. The HDTMA/HDA/TEOS/TIP molar ratio of 1/20/144/6 was used for the synthesis of the PCH-Ti sample.

2.1.4. PCH-Zr

The procedure analogous to that used for the PCH-Al synthesis was applied. The only difference was related to the use of zirconium isopropoxide (ZIP, Fluka) apart from AIP. The HDTMA/HDA/TEOS/ZIP molar ratio of 1/20/144/6 was applied the synthesis of PCH-Zr.

In the case of all PCH synthesis, in the subsequent step the modified monmorillonite samples were separated from the solutions, washed with pure ethanol, dried at room temperature and finally calcined at temperature 550 °C for 6 h.

Another two samples were obtained by modification of the as-prepared PCH-Si sample (non-calcined) with aluminum using template ion-exchange (TIE) method. 1 g of the non-calcined PCH-Si sample was introduced into 50 cm^3 of methanol solution of $Al(NO_3)_3$. Deposition of aluminum into the PCH-Si sample by TIE method was done by using two methanol solutions with $Al(NO_3)_3$ concentrations of 0.0029 and 0.0034 mol per 1 g of the non-calcined PCH sample. The slurries obtained by introduction of PCH-Si into methanol solutions of $Al(NO_3)_3$ were heated under reflux to 70 °C and intensively stirred in this temperature for next 3 h. Finally, the modified PCH-Si samples were separated by filtration, washed with methanol, dried at 60 °C and calcined at 550 °C. The samples obtained by TIE method with using less concentrated solution of $Al(NO_3)_3$ is denoted as PCH-Al(TIE1), while the sample produced with using more concentrated solution of aluminum chloride is denoted as PCH-Al(TIE2).

2.2. Characterization of catalysts

PCH materials were characterized with respect to their structure, texture, chemical composition as well as surface acidity (concentration, strength and nature of acid sites).

XRD patterns were acquired in an Empyrean diffractometer from PANalyticla, equipped with CuKα anode (λ = 0.154059). The XRD diffractograms were recorded in the 2θ range from 1 to 10° with a step of 0.01° and scan step time 200 s. In the second series of experiments the XRD patterns were recorded in the 2θ range from 5 to 70° with scan step of 0.01° and scan step time 73 s.

Textural parameters of the PCH samples were determined by N_2 adsorption at −196 °C using a 3Flex (Micromeritics) automated gas adsorption system. Prior to the analysis, the samples were outgassed under vacuum at 350 °C for 24 h. The specific surface area was determined using the BET equation, while pore size was enumerated using the DFT model. The total pore volume was determined by means of the total amount of adsorbed nitrogen at $p/p_0 = 0.98$. The micropore volume was calculated using the t-plot analysis (Harkins and Jura model).

Chemical composition of the PCH samples was determined by X-ray fluorescence (XRF) method using a Thermo Scientific ARL Quant'x spectrometer.

The form and coordination of transition metals (Fe, Ti) present in the studied samples were analyzed by UV–vis–DR spectroscopy using an Evolution 600 (Thermo) spectrophotometer. The UV–vis–DR spectra of the PCH samples were recorded in the range of 200–900 nm with a resolution of 2 nm.

The ^{27}Al MAS NMR spectrometry was used for determination of the form and coordination of aluminum species present in the samples. The spectra were collected using NMR Avance 300 MHz (Bruker) with a SB-UltraShield superconducting magnet equipped with CP/MAS probe of BL-4 type. The measurements were performed at room temperature.

The surface acidity (concentration and strength of acid sites) of the PCH materials was determined by temperature-programmed desorption of ammonia (NH_3-TPD). NH_3-TPD measurements were carried out in the temperature range of 70–550 °C in a fix bed continuous flow microreactor. The reaction temperature was measured by a K-type thermocouple located in a quartz capillary immersed in the catalyst bed. Molecules desorbing from the samples were monitored on line by a quadrupole mass spectrometer (PREVAC) connected directly to the reactor outlet via a heated line. Before NH_3-TPD experiments, the sample (100 mg) was outgassed in a flow of pure helium (20 $cm^3\ min^{-1}$) at 550 °C for 1 h. Subsequently, the sample was cooled down to 70 °C and saturated for about 2 h in a flow of NH_3 (1 vol%) diluted in He (20 $cm^3\ min^{-1}$). Then the catalyst was purged in a flow of pure helium until a constant baseline level was attained. Desorption was carried out with the linear heating rate of 10 °C min^{-1} in a flow of pure helium (20 $cm^3\ min^{-1}$). Calibration of the quadrupole mass spectrometer with commercial mixtures allowed to recalculate detector signal into ammonia desorption rate.

Distribution of acid sites of Brønsted and Lewis types was determined by FTIR analysis of the pyridine pre-adsorbed samples. Prior to FTIR studies, the samples were formed into the self-supporting wafers (ca. 5 mg cm^{-2}) and in-situ thermally treated in quartz home-made IR cell at 450 °C under high vacuum for 1 h. Quantitative experiments were carried out with the use of pyridine as a probe molecule. The measurements were realized by saturation of acid sites in the samples with pyridine (POCH) at 130 °C and subsequently, physisorbed pyridine molecules were removed by evacuation at the same temperature for 20 min and then the spectrum was recorded. FTIR spectra were recorded with a Bruker Tensor 27 spectrometer. The concentrations of both Brønsted and Lewis acid sites were calculated from the maximum intensities of the PyH^+ and PyL bands and corresponding values of the extinction coefficients (Datka et al., 1996).

2.3. Catalytic tests

The PCH samples were tested in the role of catalysts of two processes: (1) conversion of methanol to dimethyl ether (DME) and (2) conversion of ethanol to diethyl ether (DEE) and ethylene.

Catalytic experiments of both processes were performed in a fixed-bed quartz microreactor system under atmospheric pressure in the temperature range from 100 to 325 °C in intervals of 25 °C. For each test, 100 g of catalyst with a particle size between 0.160 and 0.315 mm was outgassed in a flow of pure helium at 350 °C for 1 h. After cooling down to 100 °C the gas mixture containing 3.9 vol% of methanol diluted in helium (total flow rate of 20 ml/min, isothermal saturator at 0 °C) or 5.7 vol% of ethanol diluted in pure helium (total flow rate of 20 ml/min, isothermal saturator at 20 °C) was supplied into microreactor. To avoid any condensation products during the reaction run, the gas lines were heated to 120 °C using heating tapes. The outlet gases were analyzed using a gas chromatograph (SRI 8610C) equipped with methanizer and FID detector.

For the selected catalyst additional isothermal stability tests in both studied processes were done at 250 °C for 8 h.

3. Results and discussion

Diffractograms of the PCH samples were recorded in two ranges – low 2 theta angle range (1–10°, Fig. 1A) and broad 2 theta angle range (5–70°, Fig. 1B). As in can be seen from diffractograms presented in Fig. 1A the only low intensive and broad *001* reflections, characteristic of long distance ordering of clay mineral layers were recorded in the low 2 theta angle range. Thus, the PCH samples are characterized by rather weak ordering of montmorillonite layers (partially delaminated structure). D-value determined from the locations of *001* reflections in diffractograms are in the range of 3.98–4.45 nm. Taking into account the thickness of the montmorillonite layers, which is 0.96 nm (Xu and Boyd, 1995), the interlayer distance in the PCH samples is in the range of 3.02–3.49 nm. Taking into account that length of HDTMA surfactant and HDA co-surfactant are about 2.5 nm it seems that the surfactant and co-surfactants molecules formed the paraffin-bilayer arrangement in the interlayer space of montmorillonite (Scheme 1). The possibility of the formation of such surfactant-clay mineral structure was reported by Slade and Gates (2004) and Zhu et al. (2008). However, it should be noted that this is only idealized model structure, which does not include specific interactions of surfactants with exchangeable cations, water molecules, hydrogen bonds at the mineral surface and van der Waals interactions. Experimental studies often provide only indirect information and for better understanding of this problem conjunction with atomistic models and simulation is necessary (Cygan et al., 2004a, 2004b; Heinz, 2012). Diffractograms presented in Fig. 1B are characteristic of the montmorillonite structure and also show the presence of quartz impurities in raw montmorillonite (diffractogram not shown) and therefore also in the PCH samples obtained by its intercalation. Any reflections characteristic of Al_2O_3, TiO_2 and ZrO_2 were found in diffractograms of the PCH samples, indicating deposition of these metal oxide in well dispersed forms.

Nitrogen adsorption-desorption isotherms measured for the PCH samples are shown in Fig. 2A, the profile of pore size distributions (PSD) are presented in Fig. 2B, while textural parameters of the PCH samples are compared in Table 1.

The isotherms of the PCH samples (Fig. 2A) can be classified as IVa type, according to the IUPAC recommendations (Thommes et al., 2015). This type of isotherm is characteristic of mesoporous materials. The shape of hysteresis loops differs depending on the PCH synthesis method. In the case of PCH-Si, PCH-Al, PCH-Ti and PCH-Zr hysteresis loops can be classified as H4. Such shape of hysteresis loop is characteristic of the slit-like pores with wide pore size distribution. The sharp step at the desorption branch can be attributed to pore-blocking or cavitation controlled desorption e.g. in the narrow pore "necks" of various sizes (Thommes, 2010). Deposition of aluminum by TIE method, resulting in PCH-Al(TIE1) and PCH-Al(TIE2), influenced the shape of pores in the final material, what is evidenced by the change in hysteresis shape to H3. This type of the hysteresis loop is characteristic of plate-like materials such as clays. The higher uptake at high partial pressures is connected with the presence of mesopores with greater pore diameter than in the case of the PCH-Si, PCH-Al, PCH-Ti and PCH-Zr samples (what could be also associated to the interpartical porosity).

It could be concluded that modification of PCH-Si with Al by TIE method minimized the loose in porosity and prevented pore-blocking, caused by intercalation of montmorillonite (which was followed by thermal treatment – calcination,) what is also reflected by changes in the textural properties such as BET specific surface area and pore volume (Table 1).

The PSD profiles determined by using DFT model, based on adsorption branch of isotherms, obtained for all the PCH samples consist of peaks with maximum in the range of 3.17–3.27 nm related to interlayer pores formed by pillaring process (Fig. 2B). Deposition of aluminum to as-prepared (non-calcined) PCH-Si by template ion-exchange (TIE) method resulted in slight increase in pore size in PCH-Al (TIE1) and PCH-Al(TIE2). To explain the differences in interlayer pore size of the samples obtained by TIE method and other PCHs, it should be remind that the last step of the PCH preparation is calcination of the

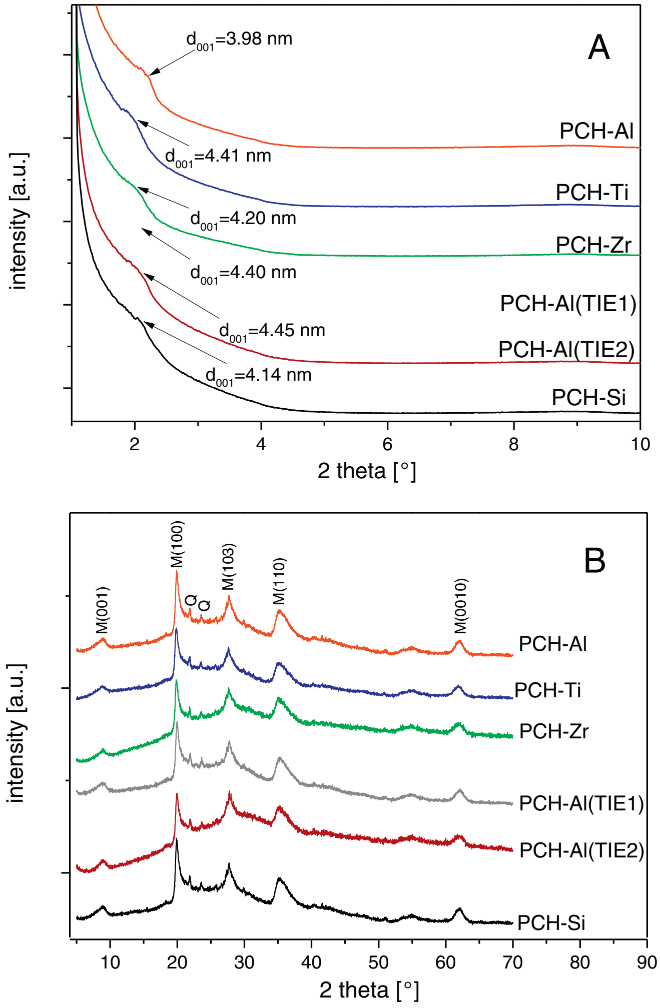

Fig. 1. X-ray diffractograms of the PCH samples recorded in low (A) and broad (B) 2 theta angle range.

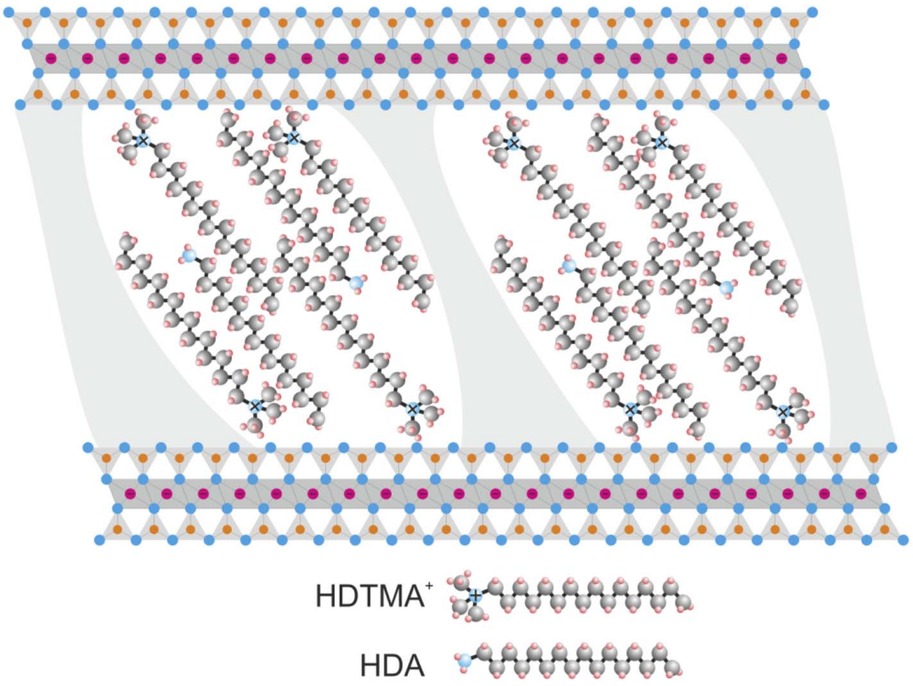

Scheme 1. Paraffin-bilayer arrangement of surfactants and co-surfactants in the interlayer space of montmorillonite.

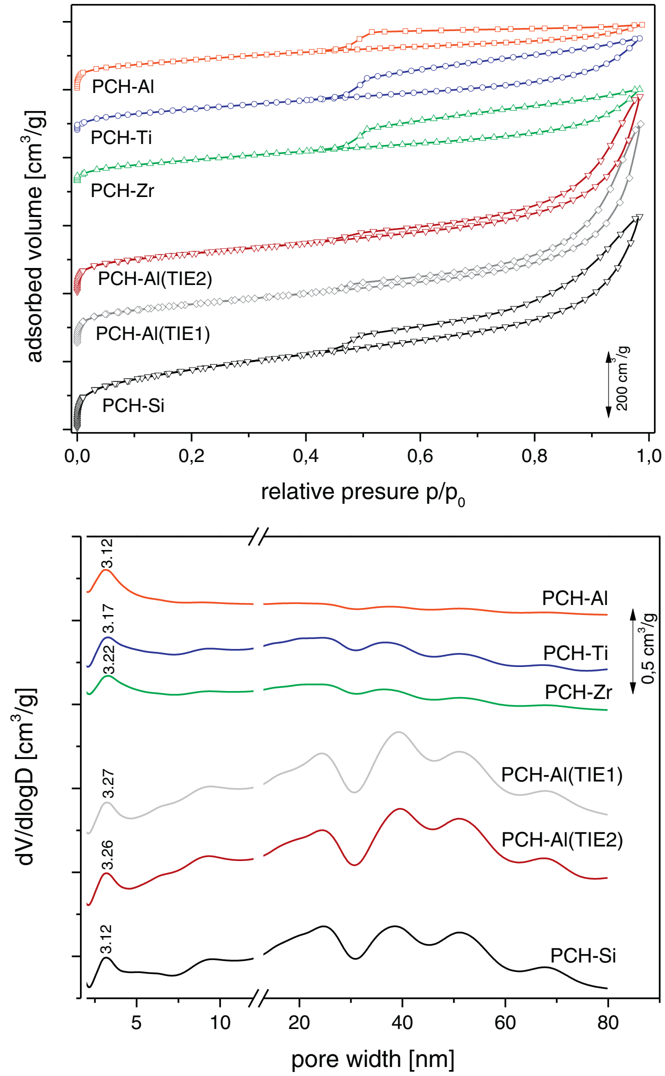

Fig. 2. Nitrogen adsorption-desorption isotherms (A) and pore size distribution (B) in the PCH samples.

Table 1
Textural parameters and surface acidity of the PCH samples.

Sample	S_{BET}	V_{TOT}	V_{mic}	CAS	DAS	Type of acid sites [%][a]	
	m^2/g	cm^3/g	cm^3/g	mmol/g	$mmol/m^2$	Brønsted	Lewis
PCH-Si	642	0.972	0.065	178	0.28	34.1	65.9
PCH-Al	318	0.296	0.002	268	0.84	30.2	69.8
PCH-Ti	338	0.466	0.001	276	0.82	48.9	51.1
PCH-Zr	320	0.387	0.004	180	0.56	50.0	50.0
PCH-Al (TIE1)	428	1.006	0.012	305	0.71	37.0	63.0
PCH-Al (TIE2)	425	0.898	0.016	306	0.72	28.1	71.9

[a] Determined by FT-IR analysis of the samples pre-adsorbed with pyridine and outgassed at 180 °C.

Table 2
Chemical composition of montmorillonite and PCH samples.

Sample	SiO_2	Al_2O_3	MgO	Fe_2O_3	CaO	K_2O	TiO_2	ZrO_2
	wt%							
Montmorillonite	69.1	21.9	3.1	3.5	0.3	0.8	0.3	0.0
PCH-Si	82.0	13.8	1.3	2.1	0.0	0.4	0.1	0.0
PCH-Al	65.5	28.6	2.0	2.9	0.1	0.6	0.2	0.0
PCH-Ti	69.9	19.0	1.9	2.1	0.1	0.5	6.3	0.0
PCH-Zr	60.9	16.2	1.2	3.2	0.2	0.6	0.2	17.3
PCH-Al(TIE1)	76.3	19.8	1.3	2.0	0.0	0.4	0.1	0.0
PCH-Al(TIE2)	75.9	20.1	1.2	2.0	0.0	0.4	0.1	0.0

as-prepared samples to remove organic templates from their pore systems. In the case of the PCH-Al(TIE1) and PCH-Al(TIE2) samples a significant amount of organic surfactants was extracted (template ion-exchange step) from the samples before calcination and therefore the heat production as a result of exothermal surfactant burning is lower in comparison to the PCH-Si, PCH-Al, PCH-Ti and PCH-Zr samples. Therefore, it could be expected that in the case of the samples obtained by TIE method their local overheating during organic templates burning is limited and therefore also collapse of the pillared structure is less significant in companion to the other PCH samples.

The interlayer distance determined from XRD studies, which is in the range of 3.02–3.49 nm (Fig. 1A) is similar to the maxima of PSD determined from the low-temperature N_2 adsorption, which is in the range of 3.12–3.27 nm (Fig. 2B).

Apart from interlayer pores, PCHs contains also larger mesopores and macropores (Fig. 2B). It can be seen that the PSD profiles in this range is very similar for PCH-Si and both samples obtained by TIE method. It is not suppressing because all these samples were obtained from this same precursor and only different methods were used for removal of surfactants from their pore systems. The PCH-Al, PCH-Ti and PCH-Zr samples are characterized by lower volume of larger pores, what could be related to deposition and partial blocking of such pores by metal Al-, Zr- and Ti-oxide aggregates.

Results of the chemical analysis of PCHs are presented in Table 2. Apart from silicon, aluminum, magnesium and iron, which are typical components of the montmorillonite layers, also small amounts of interlayer cations (Ca^{2+} and K^+), which were not completely exchange for organic surfactants during PCH synthesis, were detected. It should be mentioned that Mg^{2+} cations can be located both in the montmorillonite layers as well as interlayer cations. Small amounts of titanium were present in all PCHs as impurity of the raw clay. Intercalation of montmorillonite with Si—Ti and Si—Zr pillars resulted in increased content of these elements in the PCH samples. The mass content of deposited zirconium is nearly 3 times higher in comparison to titanium. It is related mainly to a very significant difference in their atomic mass, which is 47.9 for titanium and 91.2 for zirconium. In a group of the aluminum doped PCH samples the content of this element is significantly higher for the samples obtained by intercalation of Si—Al pillars into montmorillonite (PCH-Al) than for the samples obtained by TIE method - PCH-Al(TIE1) and PCH-Al(TIE2).

The state of aluminum in the samples was studied by ^{27}Al MAS NMR spectroscopy (Fig. 3). The spectrum of PCH-Si consists of two signals at -7 and 44 ppm corresponding to aluminum in octahedral and tetrahedral coordination, respectively (Macina et al., 2016a). Octahedral Al, with contribution of about 78% of total aluminum content, is located in octahedral sheets of montorillonite, while the remaining 22% of aluminum is in tetrahedral coordination, possibly in tetrahedral sheets of clay mineral or/and in extra-layer positions. Incorporation of aluminum into silica pillars (PCH-Al) resulted in an increase of signals related to both forms of aluminum, however the contribution of octahedrally coordinated Al was slightly lower in comparison to PCH-Si. Therefore, it seems that aluminum present in pillars of the PCH-Al sample exists both in octahedral and tetrahedral coordinations. On the other hand deposition of aluminum by using TIE method resulted mainly in surface Al in tetrahedral coordination, especially in the case of deposition of lower amounts of aluminum (PCH-Al(TIE1)), while for the sample PCH-Al(TIE2), with higher aluminum loading, this metal was also deposited in the form of octahedrally coordinated cations. Any signals

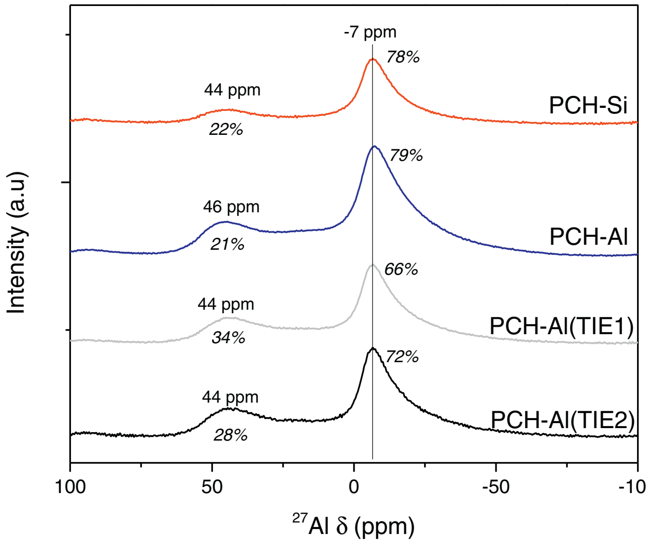

Fig. 3. The ^{27}Al MAS NMR spectra of the PCH samples doped with aluminum.

characteristic of penta-coordinated aluminum cations at about 30 ppm, which typically coexists with the signals of octahedrally and tetrahedrally coordinated Al in the spectra of Al_2O_3 aggregates (Belver et al., 2012) were found. Thus, the formation of Al_2O_3 during pillaring or TIE processes, as well as subsequent calcination was not occurred.

The forms of titanium in the PCH-Ti sample were studied by UV–vis-DR spectroscopic analysis. Because the parent montmorillonite, and therefore also all PCH materials obtained from this clay, contain iron (element active in UV–vis-DRS) the spectrum recorded for PCH-Si was subtracted from the spectrum of PCH-Ti. Such operation allows distinguishing between the bands related to iron and titanium species. The original spectrum recorded for the PCH-Si sample, deconvoluted into sub-bands, is presented in Fig. 4A. The most intensive band, assigned to iron cations in the octahedral sheets, is located at about 255 nm, while the low-intensive band at about 215 nm, could be attributed to small amount of iron incorporated into the tetrahedral sheets (Kowalczyk et al., 2016; Macina et al., 2016b). The broad band centered at about 320 nm is related to the presence of small oligomeric aggregates of iron oxides, possibly impurities of the raw clay (Kowalczyk et al., 2016; Macina et al., 2016b). Fig. 4B presents the UV–vis-DR spectrum related only to the presence of titanium in the PCH-Ti sample. The spectrum was deconvoluted into sub-bands with maxima at 235 and 270 nm. According to Chen et al. (2011) the band at about 235 nm is assigned to charge transfer from O^{2-} to Ti^{4+} in tetrahedral coordination, while the 270 nm band is attributed to charge transfer from O^{2-} to Ti^{4+} in octahedral coordination. Gianotti et al. (2003) suggest that the band at about 235 is assigned to isolated tetrahedral Ti species and small chains (a couple of tetrahedrally coordinated Ti ions linked by oxygen bridges). The band at about 270 nm indicates the presence of Ti species in octahedral coordination (possibly also Ti as penta-coordinated species), which appears upon their hydration by insertion of water molecules as extra-ligands (Galacho et al., 2007). Thus, it seems that such octahedrally coordinated Ti species are located on the surface of the interlayer pillars.

Acidity is reported to be a crucial feature of the catalysts for conversion of methanol to dimethyl ether as well as ethanol to diethyl ether and ethylene (Yaripour et al., 2005; Abu-Dahrieh et al., 2012). Therefore two experimental methods, temperature-programmed desorption of ammonia (NH_3-TPD) and FTIR analysis of the samples pre-adsorbed with pyridine (Py-FTIR), were applied for the characterization of the surface acidity of the studied samples. NH_3-TPD method allow to determine the surface concentration and relative strength of acid sites, while Py-FTIR method was used to distinguish between Lewis and Brønsted types of acid sites. NH_3-TPD profiles obtained for the PCH samples are presented in Fig. 5, while the surface concentration of acid sites (CAS) and surface density of acid sites (DAS) are compared in Table 1. It should be mentioned that the surface concentration of acid sites was determined from the NH_3-TPD experiments assuming that one ammonia molecule adsorb on one acid site. Desorption of ammonia from the PCH samples proceeded in a broad temperature range of about

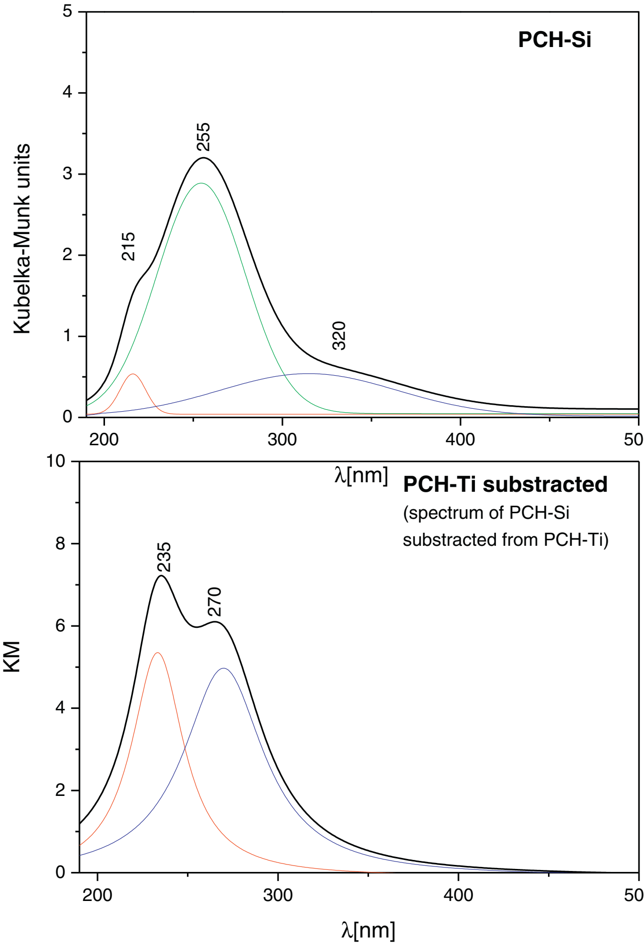

Fig. 4. The UV–vis-DR spectrum recorded for PCH-Si (A) and a result of substation of the PCH-Si spectrum from the PCH-Ti spectrum (B).

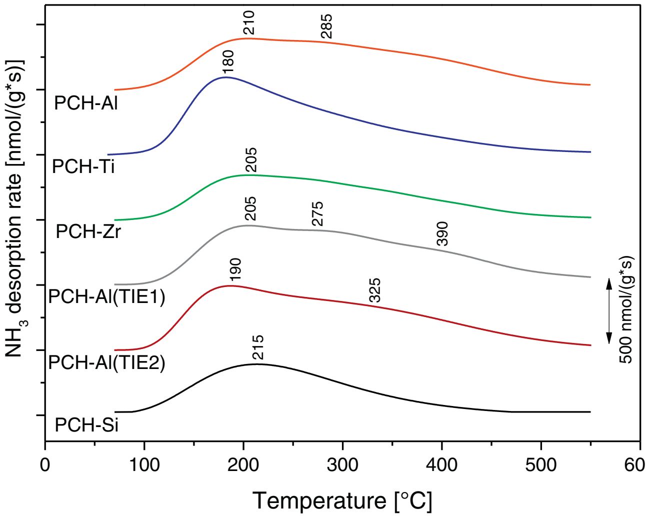

Fig. 5. NH_3-TPD profiles obtained for the PCH samples.

90–550 °C showing high heterogeneity of acid center's strength. In the case of PCHs the main desorption peak is located in the temperature range from 180 to 215 °C, what clearly shows a significant contribution of relatively weak acid sites in the samples. It should be noted that the highest temperature of the main ammonia desorption peak (215 °C) was observed for the Si-PCH sample. Assuming that in this case there are no acid sites on the pure silica pillars, the acidity of the PCH-Si sample is related only to the montorillonite layers. Incorporation of aluminum, titanium or zirconium into silica pillars shifted this maximum into lower temperatures suggesting that at least part of these metals formed acid sites of lower strength. In the case of the desorption profiles of PCH-Al and PCH-Zr the shoulders at about 250–450 °C show also the presence of stronger acid sites generated by incorporation of aluminum or zirconium into silica pillars. It proves a significant heterogeneity of strength of acid sites located on the surface of the interlayer pillars. Introduction of aluminum into the PCH-Si sample by TIE method resulted in a significant increase in its surface acidity (Table 1) as well as the formation of stronger acid sites (Fig. 5, shoulders above 250 °C). It is not surprising because in the case of the samples obtained by TIE method all introduced aluminum is deposited on the surface, in contradiction to PCH-Al, where part of aluminum is located also inside of the silica pillars. As it was shown by ^{27}Al MAS NMR analysis, a significant amount of deposited aluminum in the form of tetrahedrally coordinated species is bounded into the silica pillars. Such tetrahedrally coordinated aluminum cations in zeolites are known to form strong acid sites both Brønsted and Lewis types (Derouane et al., 2013). The formation of similar structures, of course in local scale because silica pillars, in contradiction to zeolites, have amorphous character, cannot be excluded.

The nature of acid sites was studied by FTIR spectroscopic analysis of the PCH samples adsorbed with pyridine. The recorded spectra are presented in Fig. 6, while contribution of Lewis and Brønsted acid sites in the studied samples is compared in Table 1. Interaction of Brønsted and Lewis acid sites with adsorbed pyridine resulted in an appearance of the 1545 cm^{-1} band attributed to PyH^{+} ions and 1454 cm^{-1} band, characteristic of Py-Lewis adducts. The concentration of Brønsted (PyH^{+}) and Lewis (PyL) acid sites, presented in Table 1, were calculated from the deconvoluted maximum intensities of the PyH^{+} and PyL bands and the corresponding values of the absorption coefficients: 0.078 cm μmol^{-1} and 0.16 cm μmol^{-1} (Datka et al., 1996) for the PyH^{+} and the PyL band, respectively. Pyridine also interacted with slightly acidic silanols, resulting in appearance of the 1447 cm^{-1} band (Jentys et al., 1999) (appearing for all samples) and, for the PCH-Ti and PCH-Zr samples, also with Ti^{4+} and Zr^{4+} cations, resulting in formation of the 1449 cm^{-1} maximum (Billingham et al., 1996). Analysis of the contribution of Brønsted and Lewis acidity in the PCH samples (Table 1) leads to the conclusion that montmorillonite layers in PCH-Si are characterized mainly by the presence of Lewis acids sites. Introduction of aluminum into the PCH samples, resulting in PCH-Al, PCH-Al(TIE1) and PCH-Al(TIE2), generates mainly Lewis type acid sites, while introduction of titanium (PCH-Ti) or zirconium (PCH-Zr) results in the formation mainly Brønsted type acidity.

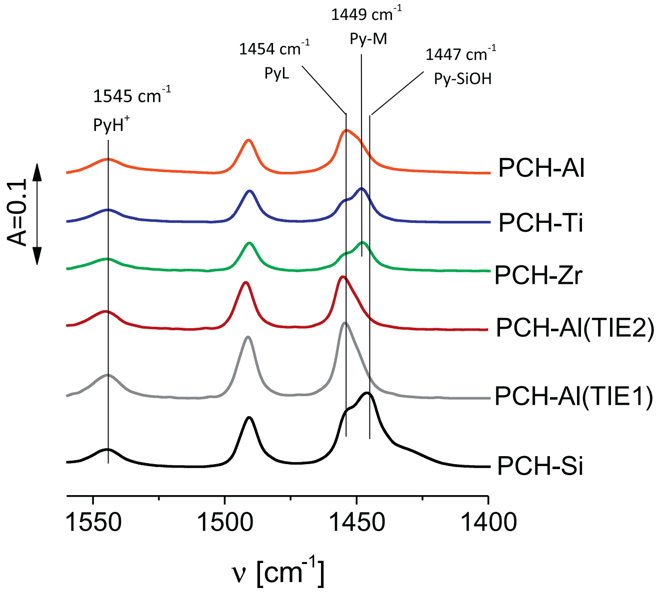

Fig. 6. FTIR spectra of the PCH samples adsorbed with pyridine.

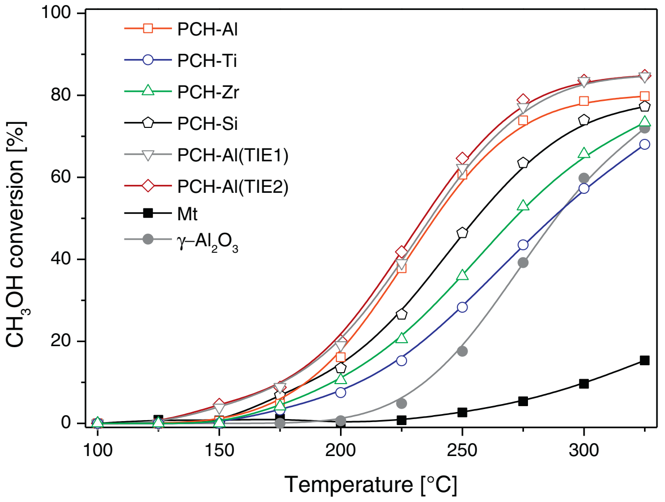

Fig. 7. Results of catalytic tests in the process of methanol to dimethyl ether dehydration over the PCH based catalysts.

The PCH samples were studied as catalysts of methanol conversion to dimethyl ether (DME) and ethanol conversion to diethyl ether (DEE) and ethylene. The results of the catalytic tests of methanol to DME conversion are presented in Fig. 7. The efficiency of this process in gas phase (without catalyst) is very limited and the methanol conversion did not excided 5% at temperature below 325 °C (results not shown). Only slightly higher methanol conversion, which reached 15% at 325 °C, was obtained in the presence of montmorillonite. Intercalation of montorillonite with silica pillars, giving the PCH-Si sample, resulted in its dramatic catalytic activation in the process of the DME synthesis. The conversion of methanol started at about 150 °C and reached 77% at 325 °C, with nearly 100% of selectivity to DME. Such significant increase in catalytic activity can be explained by opening of the interlayer space for reactants as a result of clay mineral intercalation. Assuming that in the PCH-Si sample acid sites are located only in the clay mineral layers the conversion of methanol to DME is catalyzed by these acid sites. In the case of the PCH-Ti and PCH-Zr samples the conversion of methanol started at about 150 °C and reached 68 and 73%, respectively, at 325 °C with nearly 100% selectivity to DME. Acid sites in the case of these samples are located not only in the clay mineral layers but also are related to Zr^{4+} or Ti^{4+} cations incorporated of into silica pillars. Comparison of BET specific surface area and pore volume determined for PCH-Ti, PCH-Zr and PCH-Si (Table 1), shows that in the case of two first samples pillaring was less effective and therefore also availability acid sites located in the clay mineral layers, is limited in comparison to PCH-Si. Acid sites generated by incorporation of Zr^{4+} or Ti^{4+} cations into silica pillars are characterized by lower acid strength in comparison to the sites located in the clay layers, what can be deducted from the positions of the main peaks in NH$_3$-TPD profiles (Fig. 5). It seems possible that the strength of acid sites formed by incorporation of Ti^{4+} and Zr^{4+} into silica is too low to effectively convert methanol to DME and therefore the catalytic activity of PCH-Ti and PCH-Zr is lower in comparison to PCH-Si. In contrary to titanium and zirconium, introduction of aluminum into silica pillars resulted in a significant activation of the catalyst. This effect was observed for the sample intercalated with Si—Al pillars (PCH-Al) and for the samples obtained by deposition of aluminum by TIE method - PCH-Al(TIE1) and PCH-Al(TIE2). Methanol conversion in the presence of PCH-Al started at about 150 °C and reached 80% at 325 °C (Fig. 7). The samples obtained by TIE method were more active than PCH-Al. In this case the conversion of methanol started at 125 °C, while at 325 °C reached 85% for both PCH-Al(TIE1) and PCH-Al(TIE2). Analysis of NH_3-TPD results (Fig. 5) showed that the main maxima in ammonia desorption profiles of the aluminum doped samples are located at temperatures lower in comparison to the maximum in the profile of PCH-Si. But it should be noted that deposition of aluminum, apart from the formation of relatively weak acid sites (main desorption peak), resulted also in the formation of stronger acidic sites assigned to the shoulders located in NH_3-TPD profiles at higher temperatures (275–390 °C, Fig. 5). Comparison of the Al content in the samples doped with aluminum (Table 2) showed that PCH-Al contained significantly larger amount of Al (28.5%) in comparison to the samples obtained by TIE method (about 20%). On the other hand the surface concentration of acid sites (CAS, Table 1) was higher for the samples obtained by TIE method (about 305 µmol/g) in comparison to PCH-Al (268 µmol/g). It could be explained by the formation of only surface aluminum species by TIE method, while in the case of PCH-Al part of aluminum species was located inside of silica pillars and therefore was not available for the catalysis. Thus, it seems that the synthesis of PCH-Si and subsequent deposition of aluminum by TIE method is more affective for obtaining of the active catalysts for methanol to DME conversion in comparison to the direct synthesis of PCH-Al. The TIE method resulted in catalysts with higher specific surface area and porosity and moreover, with better availability of acidic sites generated by aluminum deposition. In Fig. 7, for comparison, results of catalytic test for γ-Al_2O_3 are presented. It should be noted that PCHs modified with aluminum presented much higher catalytic activity in comparison to γ-Al_2O_3, which is commercially used for methanol to DME conversion. Thus, the PCH based catalysts seems to be very promising for application in the studied process.

Another important question is related to the role of nature acid sites and their catalytic activity in the process of methanol to DME conversion. As in can be seen from Fig. 6 and Table 1, in the case of aluminum doped samples – PCH-Al, PCH-Al(TIE1) and PCH-Al(TIE2), which were found to be the most active in a series of the studied catalysts, Lewis acid sites dominated. While in the case of PCH-Ti and PCH-Zr, which presented the lowest catalytic activity in the studied series of PCHs, significantly lower contribution of Lewis and higher contribution of Brønsted acid sites were found. Thus, it seems possible that Lewis acid sites are more catalytically active in the process of methanol to DME conversion than Brønsted acid sites. Of course this hypothesis has to be proved by additional studies.

Fig. 8 presents the results of catalytic conversion of ethanol to diethyl ether (DEE) and ethylene. The reaction seems to be similar to the described above process of ethanol to dimethyl ether, however in this case two main reaction products are formed – diethyl ether at lower reaction temperatures and ethylene at higher reaction temperatures. These temperature limits in the product formation are related to the thermodynamic constraints of ethanol conversion (de Lima et al., 2012). The ethanol conversion in the catalyst absence or in the presence of purified montmorillonite was very poor. Intercalation of montmorillonite, resulting in PCHs, very effectively activated this clay mineral for catalytic conversion of ethanol. It was related to the opening of the interlayer space of montorillonite and formation of additional acid sites by incorporation of Al, Ti and Zr into the structure of the silica interlayer pillars. The order of activity is very similar to that found for the conversion of methanol to DME (Fig. 7). In a group of the PCH samples the lowest catalytic activity presented PCH-Ti and PCH-Zr probably due to the limited efficiency of the interlayer space opening and relatively low strength of acid sites formed by incorporation of Ti or Zr into silica pillars. On the other hand, similarly to methanol conversion, the PCH samples doped with aluminum were in a group of the most active catalysts for ethanol conversion. It could be explained by generation of stronger acid sites by aluminum introduced into PCHs (Fig. 5). The difference in ethanol conversion between the reaction performed in the presence of PCH-Al and the samples obtained by TIE method (Fig. 8) is less significant in comparison to the conversion of methanol (Fig. 7).

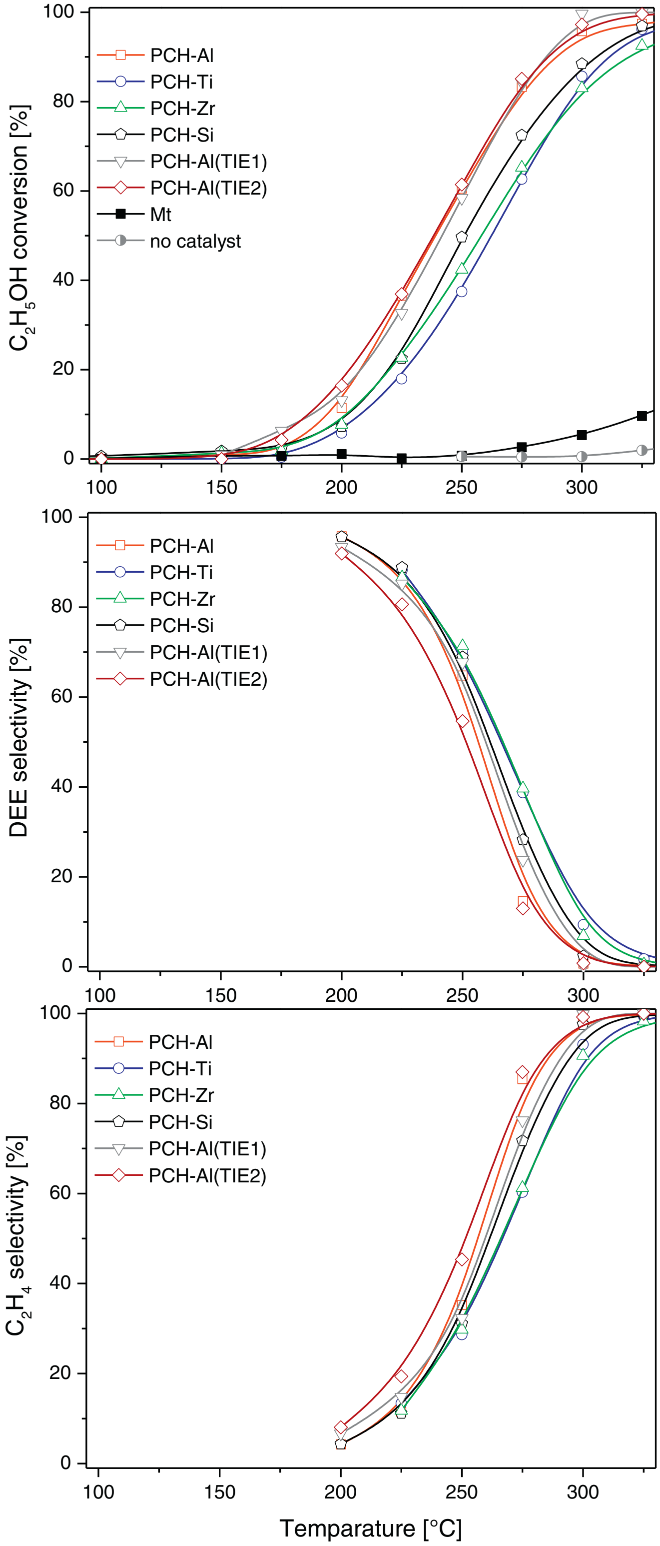

Fig. 8. Results of catalytic tests in the process of ethanol to diethyl ether and ethylene dehydration over the PCH based catalysts.

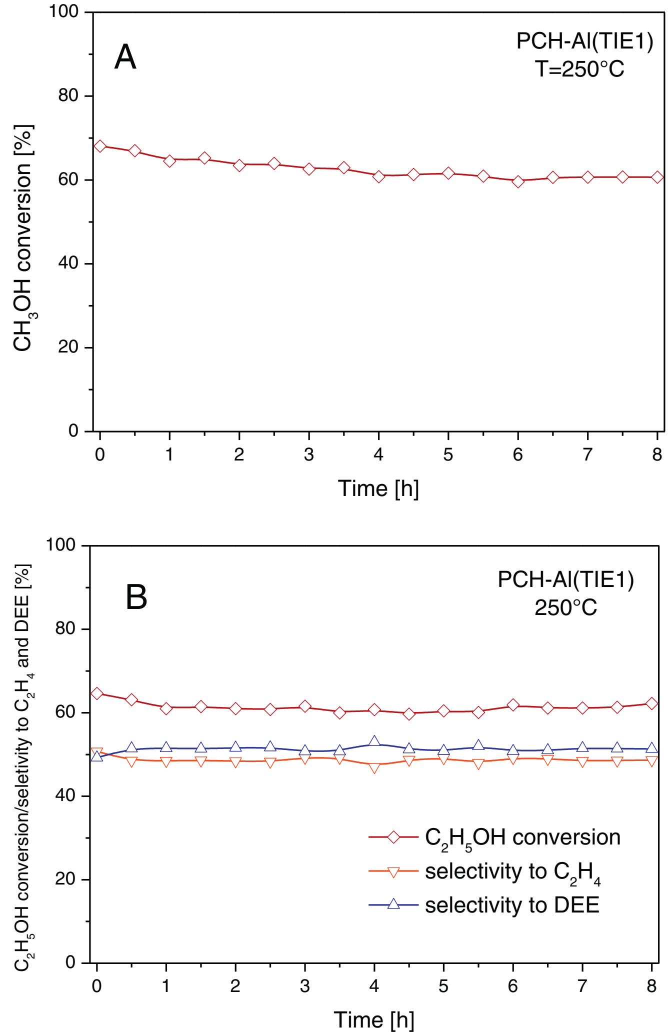

Fig. 9. Results of stability tests in the process of methanol to dimethyl ether (A) as well as ethanol to diethyl ether and ethylene over the PCH-Al(TIE1) catalysts.

DEE and ethylene were the only detected products of ethanol conversion (Fig. 8). The formation of DEE dominated in the low-temperature range. The highest selectivity to DEE was obtained in the presence of PCH-Ti and PCH-Zr, so the samples containing relatively weak acid sites with significant contribution of Brønsted type acidity. Lower selectivity to DEE presented the samples doped with aluminum - PCH-Al, PCH-Al(TIE1) and PCH-Al(TIE2), so the catalysts containing stronger acid sites mainly of Lewis type. The complete ethanol conversion with 100% selectivity to ethylene was obtained at 325 °C in the presence of the Al-doped samples - PCH-Al, PCH-Al(TIE1) and PCH-Al(TIE2). In the case of other PCHs the ethanol conversion was in the range of 85–95% at 325 °C.

The role of the acid sites nature on the alcohols dehydration reaction was studied and discussed by many authors. Recently, Phung et al. (2014), who studied dehydration of ethanol over commercial aluminas, suggested that at least part of ethanol adsorbs on the catalyst surface by replacing of hydroxyl groups (Brønsted acid sites) forming ethoxy groups and gas-phase water. Another part of ethanol is dissociatively adsorbed on Lewis acid-base pairs forming ethoxy groups and new surface OH groups. It is suggested that surface ethoxy groups are intermediate species for both diethyl ether and ethylene production. DEE is possibly formed by a nucleophilic substitution reaction where ethoxy groups attack as nucleophiles the carbon atom of either gas-phase ethanol or H-bonded adsorbed undissociated ethanol. On the other hand surface ethoxy group can be decomposed to ethylene when the concentration of available undissociated ethanol is very low. This example shows that that both Brønsted and Lewis acid sites can be catalytically active in the process of alcohol dehydration.

For the PCH-Al(TIE1) catalyst additional isothermal stability tests in both studied processes were done at 250 °C (Fig. 9). In the case of methanol dehydration the alcohol conversion dropped by about 6% from 67 to 61% during first four hours of the catalytic test and then was at nearly stable level (Fig. 9A). The ethanol conversion decreased from 64 to 61% during first hour of the catalytic test and then was stabilized on the level of 60–62% (Fig. 9B).Similarly the selectivities to ethylene and DEE were stabilized after first short period of the catalytic test. The obtained results clearly show that the studied catalyst is stable under reaction conditions.

4. Conclusions

Porous clay heterostructures (PCHs), obtained by intercalation of silica, silica-alumina, silica-titania and silica-zirconia pillars into the interlayer space of montmorillonite were characterized by high specific surface area and porosity. Incorporation of aluminum, titanium or zirconium into silica pillars resulted in lower values of these parameters in comparison to PCH intercalated with pure silica pillars (PCH-Si). Acid sites present in the montmorillonite layers and also generated by incorporation of metal (Al, Ti, Zr) species into silica pillars were catalytically active in dehydration of methanol to dimethyl ether as well as dehydration of ethanol to diethyl ether and ethylene. It was suggested that the efficiency of the PCH based catalysts depends on the strength and nature of acid sites. The best catalytic results in both studied processes were obtained of PCHs doped with aluminum, especially deposited by template ion-exchange (TIE) method, which were more catalytic active in methanol to dimethyl ether dehydration than γ-Al_2O_3 (one of the most important commercial catalysts of this process).

Acknowledgements

The studies were carried out in the frame of project 2016/21/B/ST5/00242 from the National Science Centre (Poland). Part of the research was done with equipment purchased in the frame of European Regional Development Fund (Polish Innovation Economy Operational Program - contract no. POIG.02.01.00-12-023/08).

References

Abu-Dahrieh, J., Rooney, D., Goguet, A., Saih, Y., 2012. Activity and deactivation studies for direct dimethyl ether synthesis using, CuO-ZnO-Al_2O_3 with NH_4ZSM-5, HZSM-5 or γ-Al_2O_3. Chem. Eng. J. 203, 201–211.

Aguiar, J.E., Cecilia, J.A., Tavares, P.A.S., Azevedo, D.C.S., Castellon, E.R., Lucena, S.M.P., Silva, I.J., 2017. Adsorption study of reactive dyes onto porous clay heterostructures. Appl. Clay Sci. 135, 35–44.

Alamolhoda, S., Kazemeini, M., Zaherian, A., Zakerinasab, M.R., 2012. Reaction kinetics determination and neural networks modeling of methanol dehydration over nano γ-Al_2O_3 catalyst. J. Ind. Eng. Chem. 18, 2059–2068.

Belver, C., Aranda, P., Martín-Luengo, M.A., Ruiz-Hitzky, E., 2012. New silica/alumina-clay heterostructures: properties as acid catalysts. Microporous Mesoporous Mater. 147, 157–166.

Benjelloun, M., Cool, P., Linssen, T., Vansant, E.F., 2001. Acidic porous clay heterostructures: study of their cation exchange capacity. Microporous Mesoporous Mater. 49, 83–94.

Billingham, J., Breen, C., Yarwood, J., 1996. In situ determination of Brønsted/Lewis acidity on cation-exchanged clay mineral surfaces by ATR-IR. Clay Miner. 31, 513–522.

Chen, S.-Y., Tang, C.-Y., Lee, J.-F., Jang, L.-Y., Tatsumi, T., Cheng, S., 2011. Effect of calcination on the structure and catalytic activities of titanium incorporated SBA-15. J. Mater. Chem. 21, 2255–2265.

Chmielarz, L., Kowalczyk, A., 2015. Porous clay heterostructures (PCH): synthesis and application in catalysis and adsorption. In: Aliofkhazraei, M. (Ed.), Comprehensive Guide for Mesoporous Materials, Synthesis and Characterization. vol. 1. Nova Science Publishers, New York, pp. 27–54.

Chmielarz, L., Piwowarska, Z., Kuśtrowski, P., Gil, B., Adamski, A., Dudek, B., Michalik, M., 2009a. Porous clay heterostructures (PCHs) intercalated with silica-titania pillars and modified with transition metals as catalysts for the DeNOx process. Appl. Catal. B 91, 449–459.

Chmielarz, L., Kuśtrowski, P., Piwowarska, Z., Dudek, B., Michalik, M., 2009b. Montmorillonite-based porous clay heterostructures (PCHs) intercalated with silica-titania pillars-synthesis and characterization. J. Solid State Chem. 182, 1094–1104.

Chmielarz, L., Kowalczyk, A., Michalik, M., Dudek, B., Piwowarska, Z., Matusiewicz, A., 2010. Acid-activated vermiculites and phlogophites as catalysts for the DeNOx proces. Appl. Clay Sci. 48, 156–162.

Chmielarz, L., Piwowarska, Z., Kuśtrowski, P., Węgrzyn, A., Gil, B., Kowalczyk, A., Dudek, B., Dziembaj, R., Michalik, M., 2011. Comparison study of titania pillared interlayered clays and porous clay heterostructures modified with copper and iron as catalysts of the DeNOx process. Appl. Clay Sci. 53, 164–173.

Chmielarz, L., Wojciechowska, M., Rutkowska, M., Adamski, A., Węgrzyn, A., Kowalczyk, A., Dudek, B., Boroń, P., Michalik, M., Matusiewicz, A., 2012. Acid-activated vermiculites as catalysts of the DeNOx proces. Catal. Today 191, 25–31.

Chmielarz, L., Kowalczyk, A., Wojciechowska, M., Boroń, P., Dudek, B., Michalik, M., 2014. Montmorillonite intercalated with SiO_2, SiO_2-Al_2O_3 or SiO_2-TiO_2 pillars by surfactant-directed method as catalytic supports for DeNOx process. Chem. Pap. 69, 1219–1227.

Ciftci, A., Varisli, D., Tokay, K.C., Sezgi, N.A., Dogu, T., 2012. Dimethyl ether, diethyl ether and ethylene from alcohols over tungstophosphoric acid based mesoporous catalysts. Chem. Eng. J. 207-208, 85–93.

Cygan, R.T., Guggenheim, S., van Groos, Koster, 2004a. A.F. Molecular models for the intercalation of methane hydrate complexes in montmorillonite clay. J. Phys. Chem. B 108, 15141–15149.

Cygan, R.T., Liang, J.-J., Kalinichev, A.G., 2004b. Molecular models for hydroxide, oxohydroxide, and clay phases and the development of a general force field. J. Phys. Chem. B 108, 1255–1266.

Datka, J., Gil, B., Kubacka, A., 1996. Heterogeneity of OH groups in H-mordenites: effect of dehydroxylation. Zeolites 17, 428–433.

Derouane, E.G., Védrine, J.C., Ramos Pinto, R., Borges, P.M., Costa, L., Lemos, M.A.N.D.A., Lemos, F., Ramôa Ribeiro, F., 2013. The acidity of zeolites: concepts, measurements and relation to catalysis: a review on experimental and theoretical methods for the study of zeolite acidity. Catal. Rev. 55, 454–515.

Galacho, C., Ribeiro Carrott, M.M.L., Carrott, P.J.M., 2007. Structural and catalytic properties of Ti–MCM-41 synthesised at room temperature up to high Ti content. Microporous Mesoporous Mater. 100, 312–321.

Galarneau, A., Barodawalla, A., Pinnavaia, T.J., 1995. Porous clay heterostructures formed by gallery-templated synthesis. Nature 374, 529–531.

Gianotti, E., Frache, A., Coluccia, S., Thomasc, J.M., Maschmeyer, T., Marchese, L., 2003. The identity of titanium centres in microporous aluminophosphates compared with Ti-MCM-41 mesoporous catalyst and titanosilsesquioxane dimer molecular complex: a spectroscopy study. J. Mol. Catal. A Chem. 204-205, 483–489.

Heinz, H., 2012. Clay minerals for nanocomposites and biotechnology: surface modification, dynamics and responses to stimuli. Clay Miner. 47, 205–230.

Jentys, A., Kleestorfer, K., Vinek, H., 1999. Concentration of surface hydroxyl groups on MCM-41. Microporous Mesoporous Mater. 27, 321–328.

Jin, D., Zhu, B., Hou, Z., Fei, J., Lou, H., Zheng, X., 2007. Dimethyl ether synthesis via methanol and syngas over rare earth metals modified zeolite Y and dual Cu–Mn–Zn catalysts. Fuel 86, 2707–2713.

Kito-Borsa, T., Pacas, D.A., Selim, S., Cowley, S.W., 1998. Properties of an ethanol-diethyl ether-water fuel mixture for cold-start assistance of an ethanol-fueled vehicle. Ind. Eng. Chem. Res. 37, 3366–3374.

Kooli, K., Hian, P.C., Weirong, Q., Alshahateet, S.F., Chen, F., 2006. Effect of the acid-activated clays on the properties of porous clay heterostructures. J. Porous. Mater. 13, 319–324.

Kowalczyk, A., Piwowarska, Z., Macina, D., Kuśtrowski, P., Rokicińska, A., Michalik, M., Chmielarz, L., 2016. MCM-41 modified with iron by template ion-exchange method as effective catalyst for DeNOx and NH_3-SCO processes. Chem. Eng. J. 295, 167–180.

Kowalczyk, A., Borcuch, B., Michalik, M., Rutkowska, M., Gil, B., Sojka, Z., Indyka, P., Chmielarz, L., 2017. MCM-41 modified with transition metals by template ion-exchange method as catalysts for selective catalytic oxidation of ammonia to dinitrogen. Microporous Mesoporous Mater. 240, 9–21.

de Lima, A.M., de Assis, A.J., Hori, C.E., Reis, M.H.E., Machado, A.E.H., 2012. Thermodynamic analysis of ethanol dehydration to ethylene through equilibrium constant method using classic thermodynamics and quantum chemistry, Int. Rev. Chem. Eng. 4, 466–473.

Macina, D., Piwowarska, Z., Tarach, K., Góra-Marek, K., Ryczkowski, J., Chmielarz, L., 2016a. Mesoporous silica materials modified with alumina polycations as catalysts for the synthesis of dimethyl ether from methanol. Mater. Res. Bull. 74, 425–435.

Macina, D., Piwowarska, Z., Góra-Marek, K., Tarach, K., Rutkowska, M., Girman, V., Błachowski, A., Chmielarz, L., 2016b. SBA-15 loaded with iron by various methods as catalyst for DeNOx process. Mater. Res. Bull. 78, 72–82.

Phung, T.K., Lagazzo, A., Rivero Crespo, M.A., Sanchez Escribano, V., Busca, G., 2014. A study of commercial transition aluminas and of their catalytic activity in the dehydration of ethanol. J. Catal. 311, 102–113.

Pichowicz, M., Mokaya, R., 2001. Porous clay heterostructures with enhanced acidity obtained from acid-activated clays. Chem. Commun. 2100-2101.

Pinto, M.L., Marques, J., Pires, J., 2012. Porous clay heterostructures with zirconium for the separation of hydrocarbon mixtures. Sep. Purif. Technol. 98, 337–343.

Pinto, M.L., Saini, V.K., Guil, J.M., Pires, J., 2014. Introduction of aluminum to porous clay heterostructures to modify the adsorption properties. Appl. Clay Sci. 101, 497–502.

Pires, J., Araújo, A.C., Carvalho, A.P., Pinto, M.L., González-Calbet, J.M., Ramirez-Castellanos, J., 2004. Porous materials from clays by the gallery template approach: synthesis, characterization and adsorption properties. Microporous Mesoporous Mater. 73, 175–180.

Rownaghi, A.A., Rezaei, F., Stante, M., Hedlund, J., 2012. Selective dehydration of methanol to dimethyl ether on ZSM-5 nanocrystals. Appl. Catal. B Environ. 119-120, 56–61.

Saboya, R.A.M., Cecilia, J.A., García-Sancho, C., Luna Rodríguez-Castellón, E., Cavalcante Jr., C.L., 2016. WO_3-based catalysts supported on porous clay heterostructures (PCH) with Si–Zr pillars for synthetic esters production. Appl. Clay Sci. 124–125, 69–78.

Slade, P.G., Gates, W.P., 2004. The swelling of HDTMA smectites as influenced by their preparation and layer charges. Appl. Clay Sci. 25, 93–101.

Stiefel, M., Ahmad, R., Arnold, U., Döring, M., 2011. Direct synthesis of dimethyl ether from carbon-monoxide-rich synthesis gas: influence of dehydration catalysts and operating conditions. Fuel Process. Technol. 92, 1466–1474.

Sung, D.M., Kim, Y.H., Park, E.D., Yie, J.E., 2012. Role of surface hydrophilicity of alumina in methanol dehydration. Catal. Commun. 20, 63–67.

Takahara, A., Saito, M., Inaba, M., Murata, K., 2015. Dehydration of ethanol into ethylene over solid acid catalysts. Catal. Lett. 105, 249–252.

Takeguchi, T., Yanagisawa, K., Inui, T., Inoue, M., 2000. Effect of the property of solid acid upon syngas-to-dimethyl ether conversion on the hybrid catalysts composed of Cu–Zn–Ga and solid acids. Appl. Catal. A Gen. 192, 201–209.

Thommes, M., 2010. Physical adsorption characterization of nanoporous materials. Chem. Eng. Technol. 82, 1059–1073.

Thommes, M., Kaneko, K., Neimark, A.V., Olivier, J.P., Rodriguez-Reinoso, F., Rouquerol, J., Sing, K.S.W., 2015. Physisorption of gases, with special reference to the evaluation of surface area and pore size distribution. Pure Appl. Chem. 87, 1051–1069.

Tokay, K.C., Dogu, T., Dogu, G., 2012. Methanol dehydration reaction to produce clean diesel alternative dimethyl ether over mesoporous aluminosilicate-based catalysts. Chem. Eng. J. 184, 278–285.

Varisli, D., Dogu, T., Dogu, G., 2007. Ethylene and diethyl-ether production by dehydration reaction of ethanol over different heteropoly acid catalysts. Chem. Eng. Sci. 62, 5349–5352.

Vilarrasa-Garcia, E., Cecilia, J.A., Azevedo, D.C.S., Cavalcante, C.L., Rodriguez-Castellon, E., 2017. Evaluation of porous clay heterostructures modified with amine species as adsorbent for the CO_2 capture. Microporous Mesoporous Mater. 249, 25–33.

Xu, S.H., Boyd, S.A., 1995. Cationic surfactant adsorption by swelling and nonswelling layer silicates. Langmuir 11, 2508–2514.

Xu, M., Lunsford, J.H., Goodman, D.W., Bhattacharyya, A., 1997. Synthesis of dimethyl ether (DME) from methanol over solid-acid catalysts. Appl. Catal. A Gen. 149, 289–301.

Yaripour, F., Baghaei, F., Schmidt, I., Perregaard, J., 2005. Catalytic dehydration of methanol to dimethyl ether (DME) over solid-acid catalysts. Catal. Commun. 6, 147–152.

Zhu, R., Zhu, L., Zhu, J., Xu, L., 2008. Structure of cetyltrimethylammonium intercalated hydrobiotite. Appl. Clay Sci. 42, 224–231.